Supplementary material

Content

i. Tables

ii. Figures

- **Supplementary Figure 5 (page 23)**

Comparison of abundance of immune and stromal cell populations in the pGBM molecular subtypes (exploratory cohort).

- **Supplementary Figure 6 (page 24)**

Molecular characterization of the pGBM-I1 and pGBM-I2 clusters according to the Verhaak’s signatures in the validation dataset.

- **Supplementary Figure 7 (page 25)**

Heatmaps of MCPcounter scores in mesenchymal tumors of the exploratory cohort.

- **Supplementary Figure 8 (page 26)**

Heatmaps of MCPcounter scores in neural tumors of the exploratory cohort.

- **Supplementary Figure 9 (page 27)**

Heatmaps of MCPcounter scores in classical tumors of the exploratory cohort.

- **Supplementary Figure 10 (page 28)**

Heatmaps of MCPcounter scores in proneural tumors of the exploratory cohort.

- **Supplementary Figure 11 (page 29)**

Kaplan-Meier curves modeling the effect of GBM molecular classification on survival in the validation cohort.

- **Supplementary Figure 12 (page 30)**

Kaplan-Meier curves modeling the effect of tumor infiltration on overall survival in the validation cohort.

- **Supplementary Figure 13 (pages 31)**

Effect of molecular subtypes on survival, in the pooled exploratory and validation cohorts, in (A) pGBM-I1 and (B) pGBM-I2.

Sample ID	**Gender**	**Age**[c]	**Histopathological diagnosis**	**WHO grade**	***IDH1/IDH2* status**	**Combined +7-10**[d]	**LOH 1p/19q**	***MGMT* promoter methylation**[e]
06-1563[a]	Male	35	A	II	MUT	NA	No	U/M
07-0658	Male	25	A	II	MUT	NA	No	U/M
07-0841	Male	32	A	II	MUT	NA	No	NA
07-1082	Male	28	A	II	MUT	NA	No	U/M
08-0706	Female	42	A	II	MUT	NA	No	U/M
08-1168	Female	43	A	II	MUT	NA	No	U/M
08-1169	Male	37	A	II	MUT	NA	No	M/M
1002-0669	Male	31	A	II	MUT	NA	No	NA
07-0025	Male	64	A	II	MUT	NA	No	U/M
07-0041[b]	Female	29	A	II	MUT	NA	No	U/M
07-0139	Male	40	A	II	MUT	NA	No	M/M
07-0350	Male	35	A	II	MUT	NA	No	M/M

07-0372	Female	32	A	II	MUT	NA	No	M/M
07-0450	Male	36	O	II	MUT	NA	Yes	M/M
07-0697	Male	51	A	II	MUT	NA	No	M/M
08-1321	Female	41	A	II	MUT	NA	No	NA
08-1498	Female	61	A	II	MUT	NA	No	U/M
08-1510	Male	38	A	II	MUT	NA	No	U/M
08-1592	Male	55	O	II	MUT	NA	Yes	M/M
06-1206	Female	36	O	II	MUT	NA	Yes	M/M
06-1467	Female	30	O	II	MUT	NA	Yes	U/M
07-0704	Male	45	O	II	MUT	NA	Yes	U/M
07-1341	Male	23	O	II	MUT	NA	Yes	U/M
07-1656	Female	51	A	II	WT	NA	No	U/U
09-0349	Female	36	O	II	NA	NA	Yes	NA
1002-0413	Female	40	O	II	MUT	NA	Yes	NA
06-0811	Male	70	pGBM	IV	WT	NA	NA	U/U
06-0813	Female	82	pGBM	IV	NA	NA	NA	NA
06-0823	Male	76	pGBM	IV	WT	Yes	NA	M/M

06-0849	Male	56	pGBM	IV	WT	Yes	NA	U/U
06-0984	Male	63	pGBM	IV	WT	No	NA	M/M
06-1051	Male	61	pGBM	IV	WT	Yes	NA	U/U
06-1126	Female	59	pGBM	IV	WT	Yes	NA	M/M
06-1163	Female	84	pGBM	IV	NA	NA	NA	NA
06-1277	Male	70	pGBM	IV	WT	Yes	NA	U/U
06-1471	Female	79	pGBM	IV	WT	No	NA	M/M
06-1591	Female	58	pGBM	IV	WT	Yes	NA	U/M
06-1603	Male	53	pGBM	IV	WT	Yes	NA	U/M
07-0173	Female	46	pGBM	IV	WT	Yes	NA	U/U
07-0666	Male	58	pGBM	IV	NA	No	NA	NA
07-0860	Male	65	pGBM	IV	WT	Yes	NA	U/U
07-0968	Male	62	pGBM	IV	WT	Yes	NA	U/M
07-1024	Male	81	pGBM	IV	WT	NA	NA	NA
07-1380	Male	70	pGBM	IV	WT	Yes	NA	M/M
07-1562	Male	56	pGBM	IV	WT	NA	NA	U/U
07-1568	Male	55	pGBM	IV	WT	No	NA	M/M

08-0123	Female	54	pGBM	IV	WT	NA	NA	M/M
08-0193	Male	48	pGBM	IV	WT	NA	NA	U/U
08-0194	Female	65	pGBM	IV	WT	NA	NA	M/M
08-0269	Male	59	pGBM	IV	WT	NA	NA	U/U
08-0308	Female	36	pGBM	IV	WT	NA	NA	U/U
08-0315	Female	61	pGBM	IV	WT	NA	NA	M/M
08-0316	Female	81	pGBM	IV	WT	NA	NA	NA
08-0417	Female	63	pGBM	IV	WT	NA	NA	M/M
08-0723	Female	56	pGBM	IV	WT	NA	NA	U/U
08-1253	Male	50	pGBM	IV	WT	NA	NA	U/U
08-1516	Male	81	pGBM	IV	WT	NA	NA	U/U
08-1556	Male	75	pGBM	IV	WT	NA	NA	U/U
09-0133	Male	55	pGBM	IV	WT	NA	NA	M/M
09-0201	Female	67	pGBM	IV	WT	NA	NA	NA
0992-0111	Female	82	pGBM	IV	WT	NA	NA	NA
0992-0314	Female	56	pGBM	IV	WT	NA	NA	NA
06-1223	Male	46	sGBM	IV	MUT	Yes	NA	M/M

07-0196	Male	48	sGBM	IV	MUT	NA	NA	U/M
08-0243	Female	38	sGBM	IV	MUT	NA	NA	NA
09-0194 [a]	Male	38	sGBM	IV	MUT	NA	NA	NA
09-0380 [b]	Female	32	sGBM	IV	MUT	NA	NA	NA

[a] Samples originate from the same patient. [b] Samples originate from the same patient. [c] Age in years, [d] combined gain of chromosome 7 and loss of chromosome 10 (+7/-10) [e] Methylation status as determined by qMSP and Pyrosequencing (qMSP result / pyrosequencing result).

Supplementary Table 1: Summary of in-house patient characteristics (n = 67).

Gene	**Regulation in pGBM-I1** (*vs.* Normal, FDR<0.05)	**Regulation in pGBM-I2** (*vs.* Normal, FDR<0.05)	**Regulation in pGBM-I1** (*vs.* pGBM-I2, FDR<0.05)
VEGFA	-	-	**Up**
IL10	**Up**	-	**Up**
IL23A	-	-	**Up**
TGFB1	**Up**	-	**Up**
SPATA2	**Down**	**Down**	-
PDL1/CD274	-	-	**Up**
CTLA4	-	-	**Up**
CSF1	**Up**	-	**Up**
CCL2	**Up**	-	**Up**
CCL22	-	-	**Up**
CD163	**Up**	-	**Up**
MSR1	**Up**	-	**Up**

GDF15	-	-	Up
ARG1	-	Down	-
CD47	-	-	-
IL6	-	-	Up
IL6ST	Up	Up	-
JAK2	-	-	-
STAT3	Up	Up	Up
PIM1	-	-	Up
SOCS3	-	-	Up
STAT5A	-	-	Up
STAT5B	-	-	Down
CD4	Up	-	Up
ICOS	-	-	Up
FOXP3	-	-	Up

Supplementary Table 2: Regulation of immune suppressor genes in the pGBM infiltration clusters of the exploratory cohort.

Gene	**Regulation in pGBM-I1** (*vs.* Normal, FDR<0.05)	**Regulation in pGBM-I2** (*vs.* Normal, FDR<0.05)	**Regulation in pGBM-I1** (*vs.* pGBM-I2, FDR<0.05)
IFN-γ	-	-	**Up**
IL1A	-	-	**Up**
IL2	-	-	-
IL4	-	-	-
IL7	-	-	**Up**
IL12A	-	-	**Down**
IL15	-	-	**Up**
TNF	-	-	**Up**
CD3D	-	-	**Up**
CD8A	-	-	**Up**
CD8B	-	-	**Up**
CD80	-	-	**Up**
CD86	**Up**	-	**Up**

CD40	-	-	**Up**
HLA-B	**Up**	-	**Up**
HLA-DRA	**Up**	-	**Up**
HLA-DBP1	**Up**	-	**Up**
B2M	**Up**	**Up**	-
RELA	**Up**	**Up**	**Up**
STAT1	-	**Up**	**Down**
IRAK1	**Up**	-	**Up**
STAT4	**Down**	**Down**	**Up**
TBX21	-	-	**Up**
CD226	**Up**	-	**Up**
IRF7	-	-	**Up**
NCR1	-	-	**Up**
NCR3	-	-	**Up**
NCR2	-	-	**Up**

KLRD1	-	-	Up
CD244	-	-	Up
TLR2	Up	-	Up
TLR3	Up	Up	-
TLR4	-	-	Up
TLR9	-	-	Up
TREM1	Up	-	Up
TREM2	Up	-	Up
MIF	-	-	Up

Supplementary Table 3: Regulation of immune effector genes in the pGBM infiltration clusters of the exploratory cohort.

		Patients (n)	Events (n)	Univariable models HR (95% CI)	 *p*-value	Multivariable model HR (95% CI)	 *p*-value
Molecular classif.				*p*-value of the model: 0.086			
	Classical	113	73	-		1.00 (ref)	
	Mesenchymal	137	101	-		1.71 (1.23-2.39)	**0.0016**
	Neural	73	52	-		1.21 (0.85-1.73)	0.29
	Proneural	105	75	-		1.34 (0.97-1.86)	0.080
Immune classif.				*p*-value of the model: 0.032			
	pGBM-I1	192	130	1.00 (ref)		1.00 (ref)	
	pGBM-I2	236	171	1.29 (1.02-1.61)	**0.032**	1.51(1.14-2.00)	**0.0037**

Supplementary Table 4: Univariable and multivariable Cox's proportional hazard analyses, with survival as endpoint, in the exploratory cohort.

				Univariable models		Multivariable model	
		Patients (n)	Events (n)	HR (95% CI)	*p*-value	HR (95% CI)	*p*-value
Molecular classif.				*p*-value of the model: 0.033			
	Classical	32	21	1.00 (ref)		1.00 (ref)	
	Mesenchymal	35	27	1.02 (0.58-1.81)	0.94	1.30 (0.70-2.43)	0.41
	Neural	29	16	0.60 (0.31-1.15)	0.12	0.61 (0.32-1.18)	0.15
	Proneural	28	12	0.42 (0.21-0.86)	**0.018**	0.39 (0.19-0.80)	**0.010**
Immune classif.				*p*-value of the model: 0.47			
	pGBM-I1	57	35	-		1.00 (ref)	
	pGBM-I2	67	41	-		1.69 (1.00-2.84)	**0.048**

Supplementary Table 5: Univariable and multivariable Cox's proportional hazard analyses, with survival as endpoint, in the validation cohort.

				Univariable models		Multivariable model	
		Patients (n)	Events (n)	HR (95% CI)	*p*-value	HR (95% CI)	*p*-value
Molecular classif.				*p*-value of the model: 0.17			
	Classical	145	94	-		1.00 (ref)	
	Mesenchymal	172	128	-		1.63 (1.21-2.18)	**0.0012**
	Neural	102	68	-		1.09 (0.80-1.49)	0.59
	Proneural	133	87	-		1.09 (0.81-1.47)	0.57
Immune classif.				*p*-value of the model: 0.025			
	pGBM-I1	249	165	1.00 (ref)		1.00 (ref)	
	pGBM-I2	303	212	1.26 (1.03-1.55)	**0.025**	1.55 (1.21-1.97)	**4.8e-4**
Cohort				*p*-value of the model: 0.0022			
	In-house	36	30	1.00 (ref)		1.00 (ref)	
	TCGA	392	271	0.075 (0.49-1.04)		0.76 (0.51-1.11)	0.15
	Rembrandt	124	76	0.0013 (0.33-0.76)		0.53 (0.34-0.82)	**0.0043**

Supplementary Table 6: Univariable and multivariable Cox's proportional hazard analyses, with survival as endpoint, in the pooled exploratory and validation cohorts.

	pGBM-I1				pGBM-I2			
	Patients (n)	Events (n)	HR (95% CI)	*p*-value	Patients (n)	Events (n)	HR (95% CI)	*p*-value
Molecular classif.								
Classical	51	30	1.00 (ref)		94	64	1.00 (ref)	
Mesenchymal	140	100	1.55 (1.03-2.33)	**0.037**	32	28	1.81 (1.15-2.86)	**0.011**
Neural	34	18	0.87 (0.48-1.57)	0.64	68	50	1.19 (0.82-1.73)	0.36
Proneural	24	17	1.52 (0.84-2.78)	0.17	109	70	1.02 (0.73-1.44)	0.90
Cohort								
In-house	19	15	1.00 (ref)		17	15	1.00 (ref)	
TCGA	173	115	0.70 (0.41-1.19)	0.19	219	156	0.84 (0.48-1.47)	0.55
Rembrandt	57	35	0.52 (0.28-0.96)	**0.037**	67	41	0.56 (0.30-1.04)	0.066

Supplementary Table 7: Effect of molecular subtypes on survival in pGBM-I1 and pGBM-I2, in the pooled exploratory and validation cohorts.

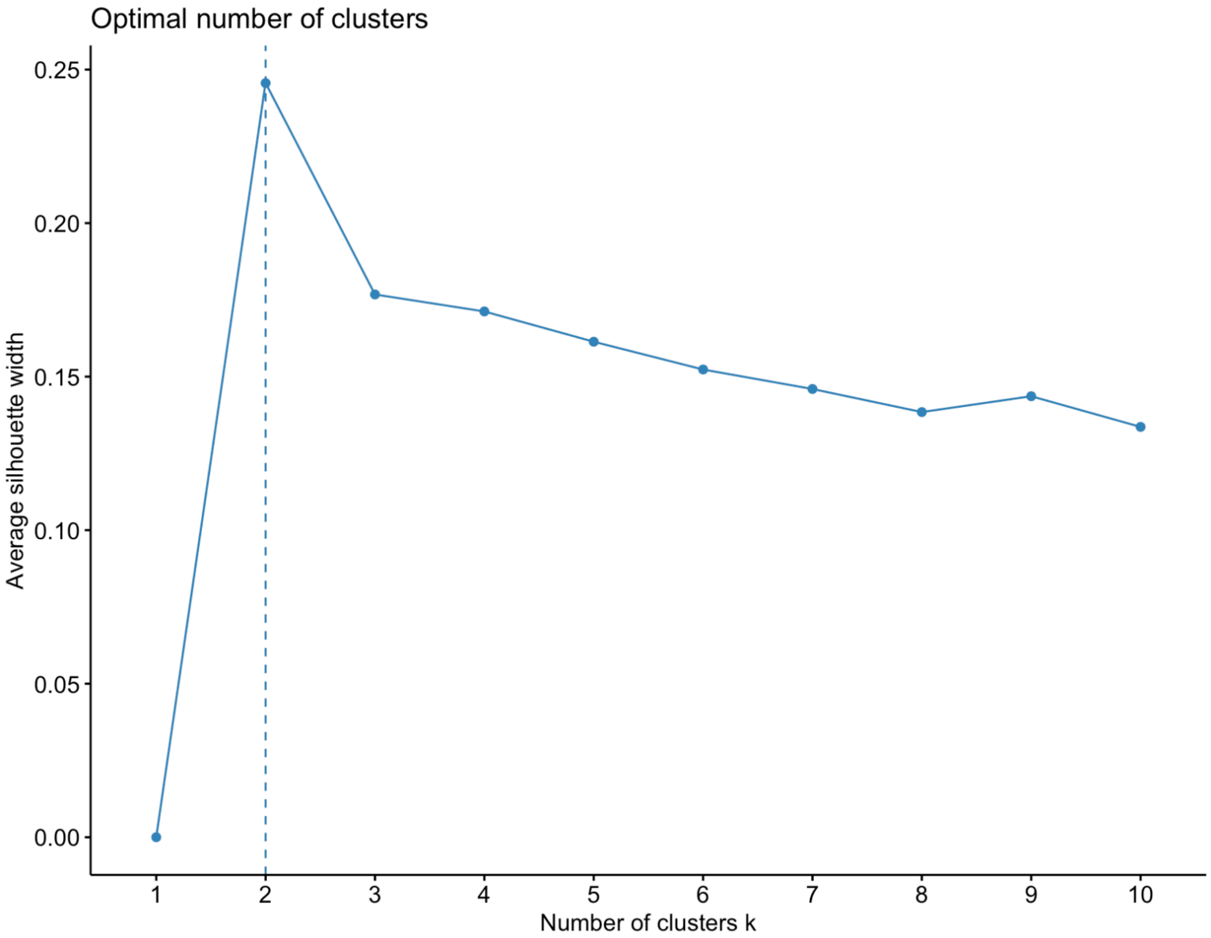

Supplementary Figure 1: Selection of the number of pGBM infiltration clusters in the exploratory cohort. The silhouette plot identifies the optimal number of clusters, which maximizes the average silhouette width over a range of possible values (k = 1 to 10).

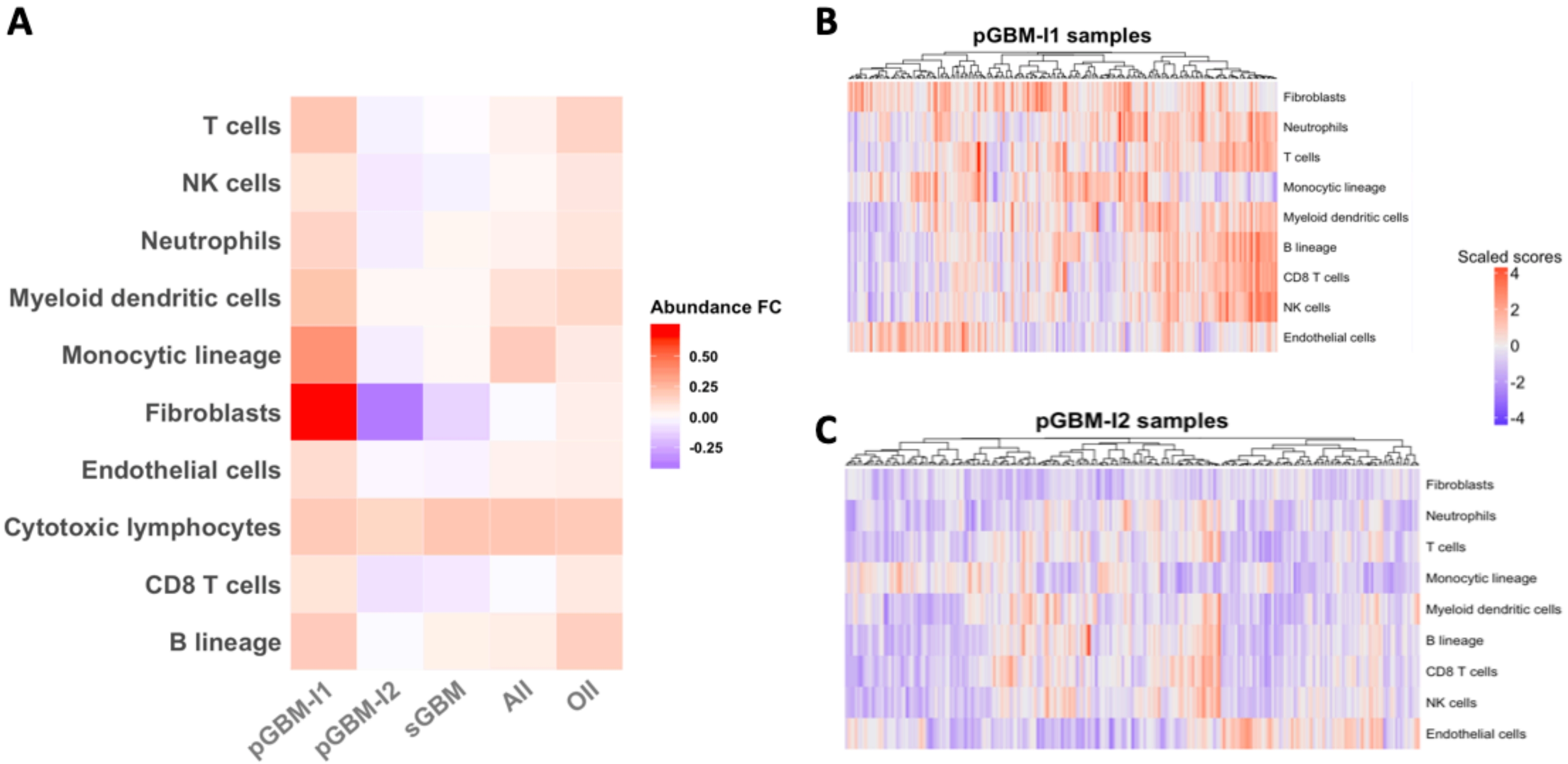

Supplementary Figure 2: Estimation of tumor infiltration across samples of the exploratory cohort. (A) Abundance fold-changes (FC), *i.e.* average infiltration scores in tumors - averages infiltration score in normal samples. Red color indicates a higher infiltration in tumors, compared to normal, while blue color underlines a lower infiltration in tumors. Heatmaps of MCPcounter scores in (B) pGBM-I1 and (C) pGBM-I2 samples. Columns are ordered using a hierarchical clustering procedure, using 1-Pearson's correlation as a measure of distance between samples.

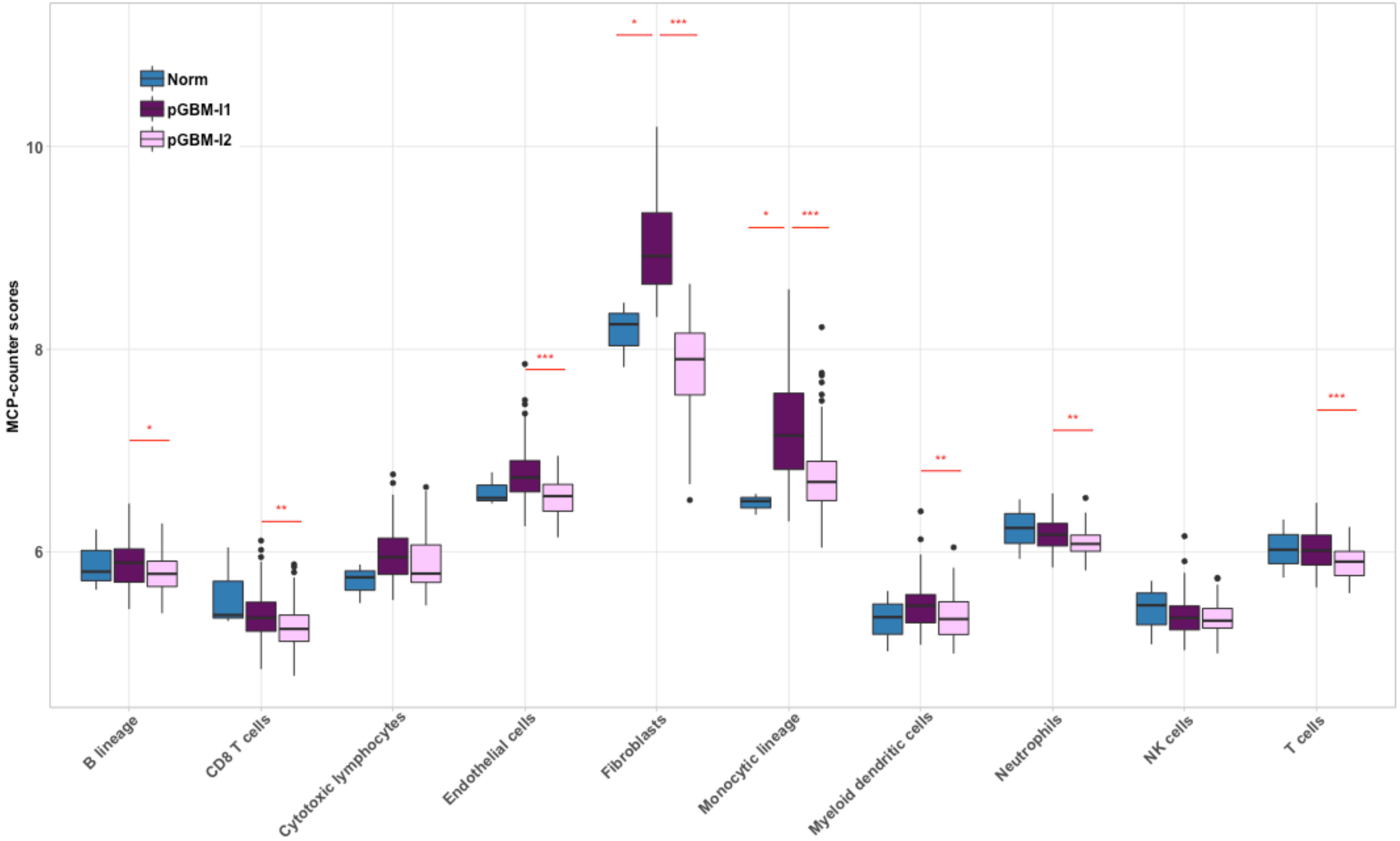

Supplementary Figure 3: Differential abundance of immune and stromal cell populations between pGBM-I1 (n=57) and pGBM-I2 (n=67), in the validation dataset. FDR values from limma (Benjamini-Hochberg procedure) are indicated for each comparison. Legend: (*) FDR<0.05, (**) FDR<0.01, (***) FDR<0.001.

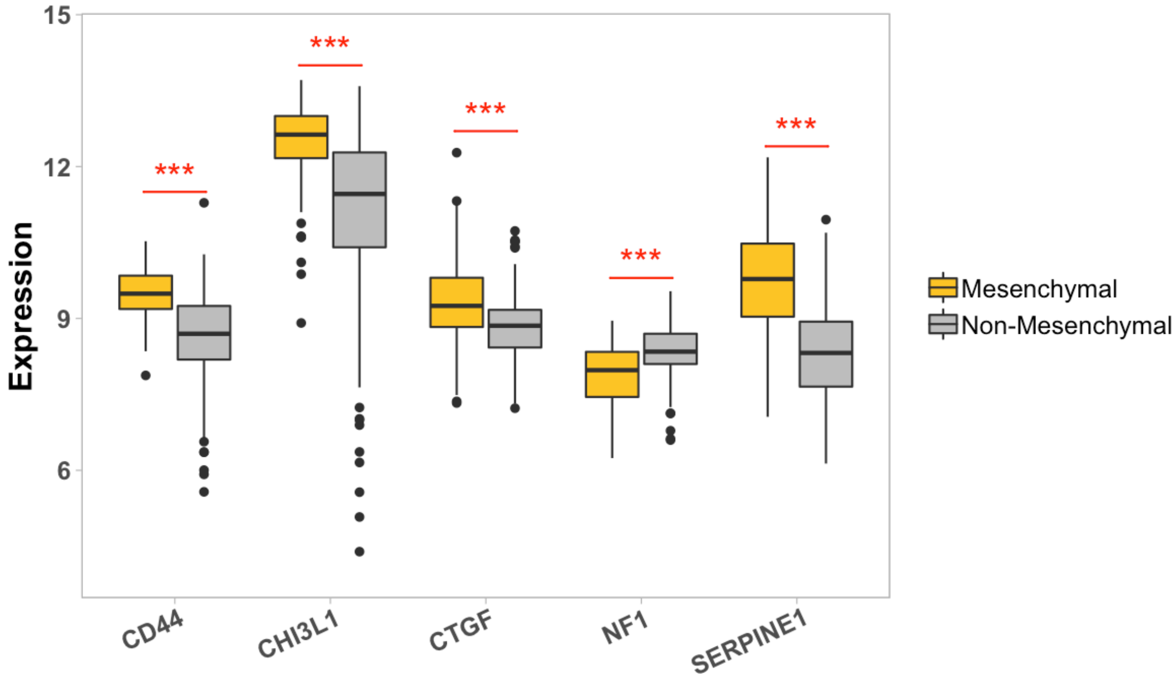

Supplementary Figure 4: Expression levels of selected genes in the mesenchymal subtype *vs.* other subtypes (neural, proneural and classical) in the exploratory cohort. FDR values from limma (Benjamini-Hochberg procedure) are indicated for each comparison. Legend: (*) FDR<0.05, (**) FDR<0.01, (***) FDR<0.001.

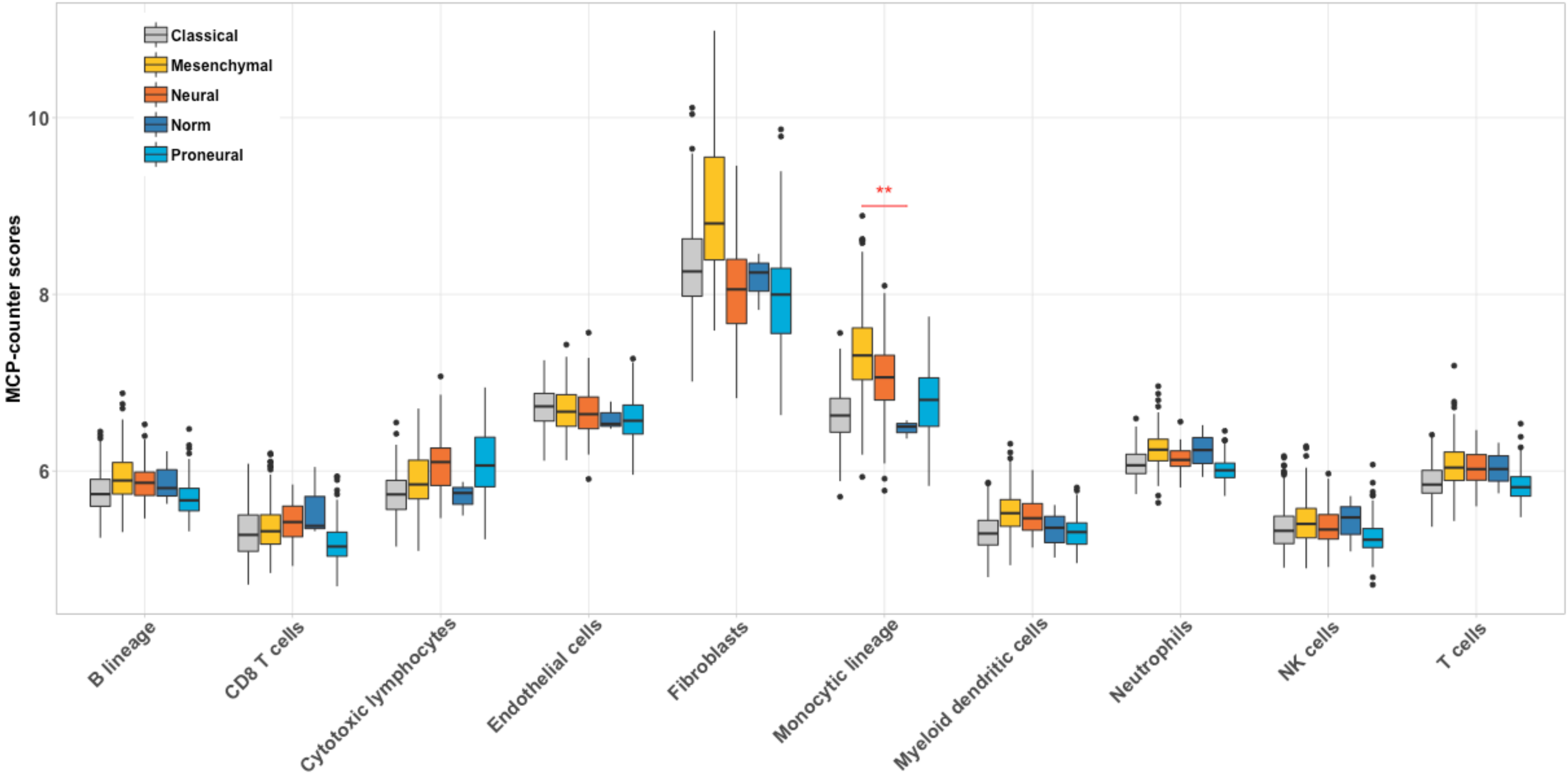

Supplementary Figure 5: Comparison of abundance of immune and stromal cell populations in the pGBM molecular subtypes (exploratory cohort).

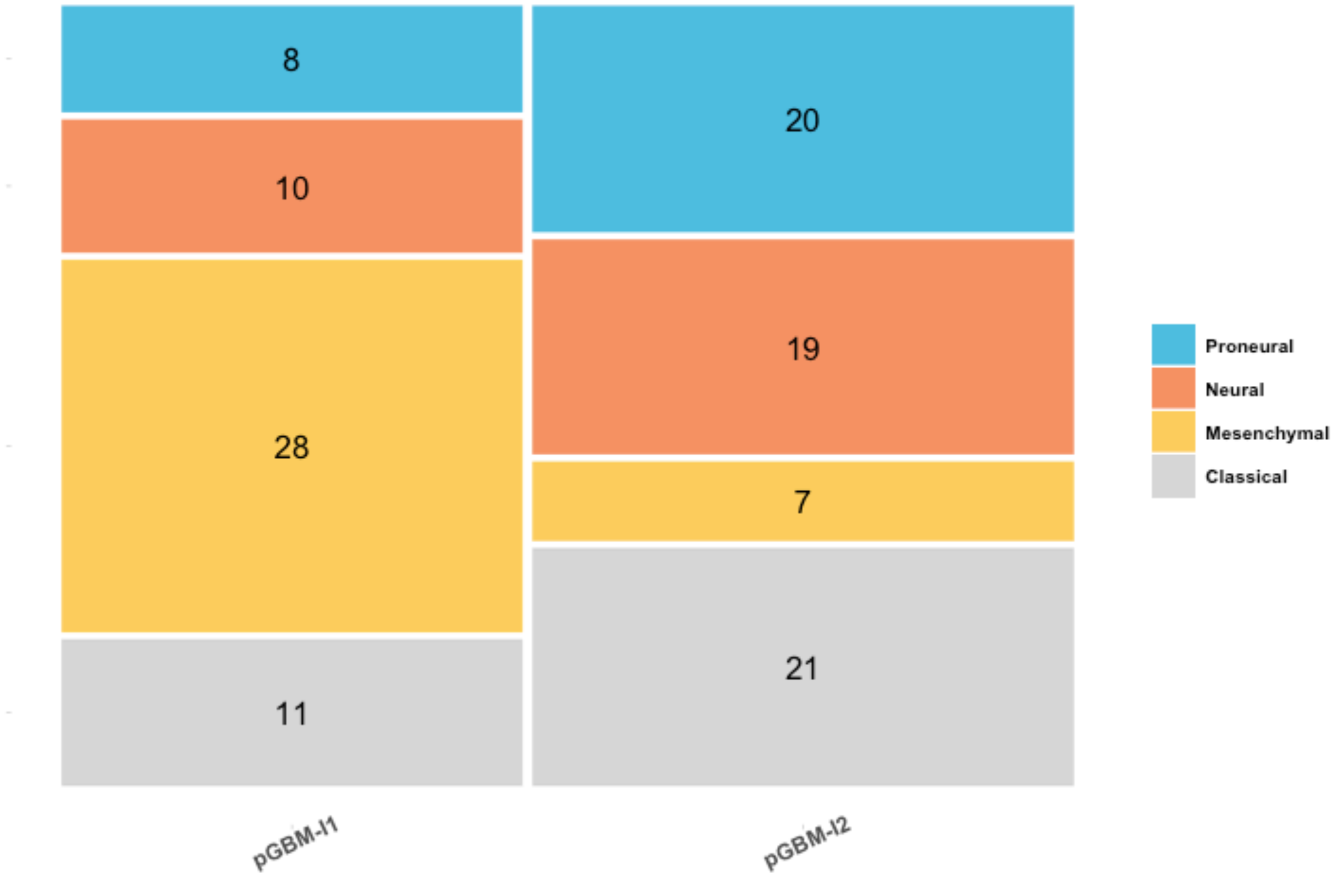

Supplementary Figure 6: Molecular characterization of the pGBM-I1 (n=57) and pGBM-I2 (n=67) clusters according to the Verhaak's signatures in the validation dataset.

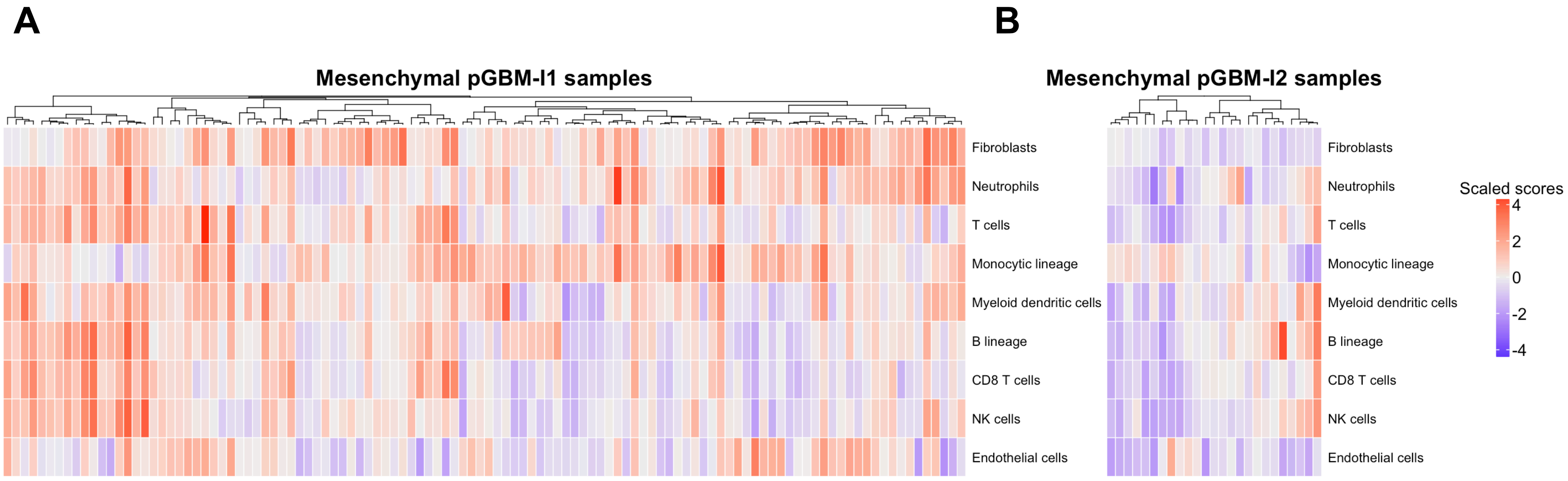

Supplementary Figure 7: Heatmaps of MCPcounter scores in mesenchymal tumors of the exploratory cohort (A) pGBM-I1 and (B) pGBM-I2. Columns are ordered using a hierarchical clustering procedure, using 1-Pearson's correlation as a measure of distance between samples.

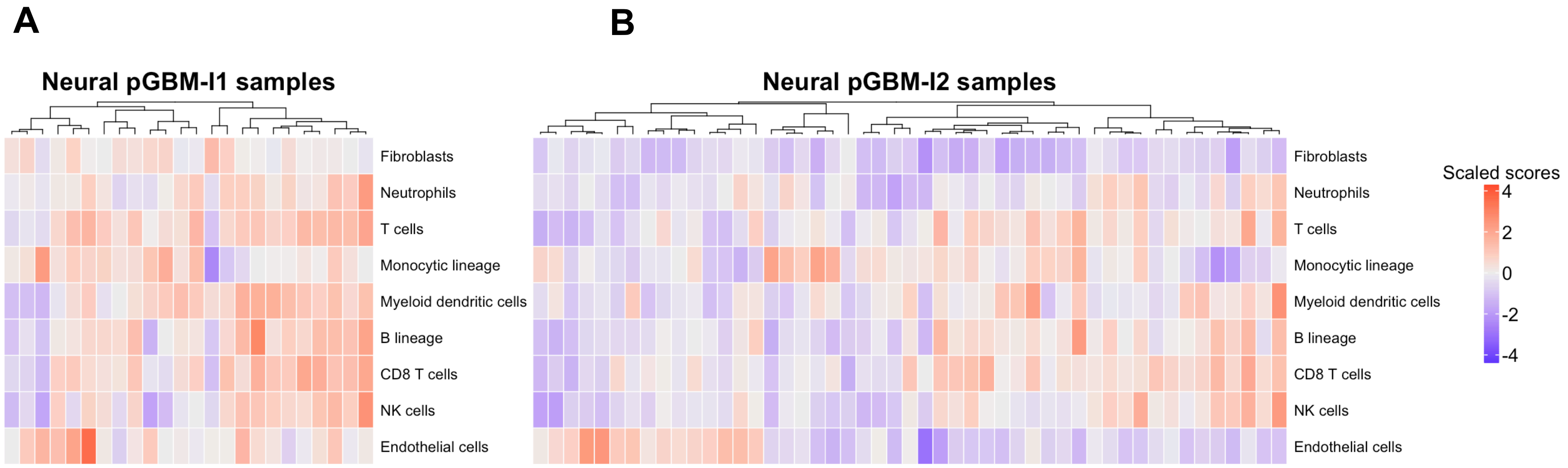

Supplementary Figure 8: Heatmaps of MCPcounter scores in neural tumors of the exploratory cohort (A) pGBM-I1 and (B) pGBM-I2. Columns are ordered using a hierarchical clustering procedure, using 1-Pearson's correlation as a measure of distance between samples.

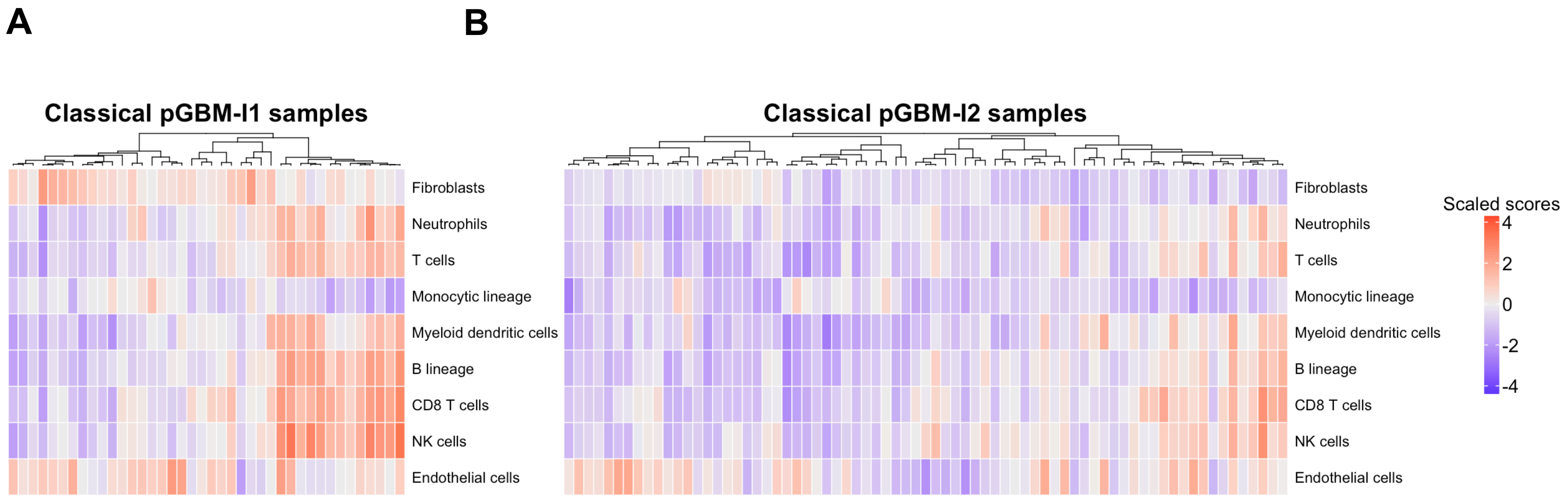

Supplementary Figure 9: Heatmaps of MCPcounter scores in classical tumors of the exploratory cohort (A) pGBM-I1 and (B) pGBM-I2. Columns are ordered using a hierarchical clustering procedure, using 1-Pearson's correlation as a measure of distance between samples.

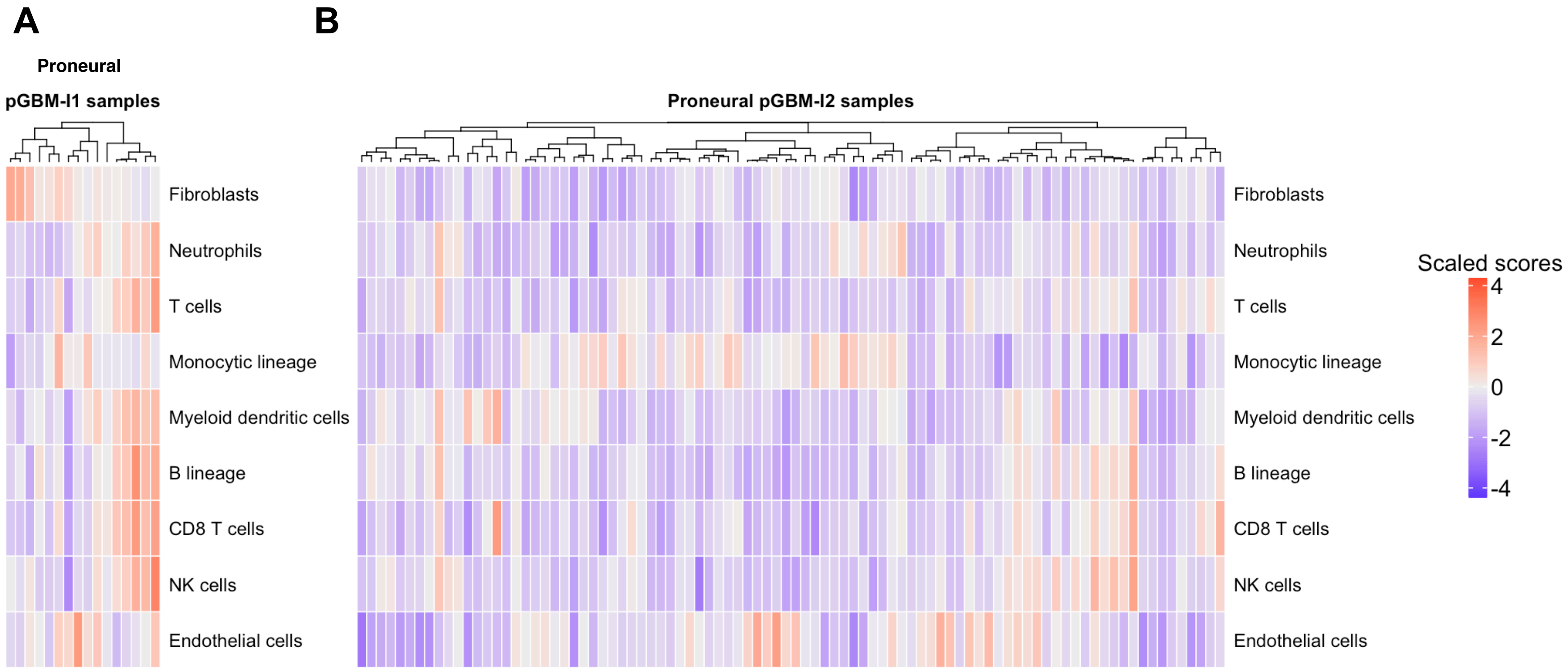

Supplementary Figure 10: Heatmaps of MCPcounter scores in proneural tumors of the exploratory cohort (A) pGBM-I1 and (B) pGBM-I2. Columns are ordered using a hierarchical clustering procedure, using 1-Pearson's correlation as a measure of distance between samples.

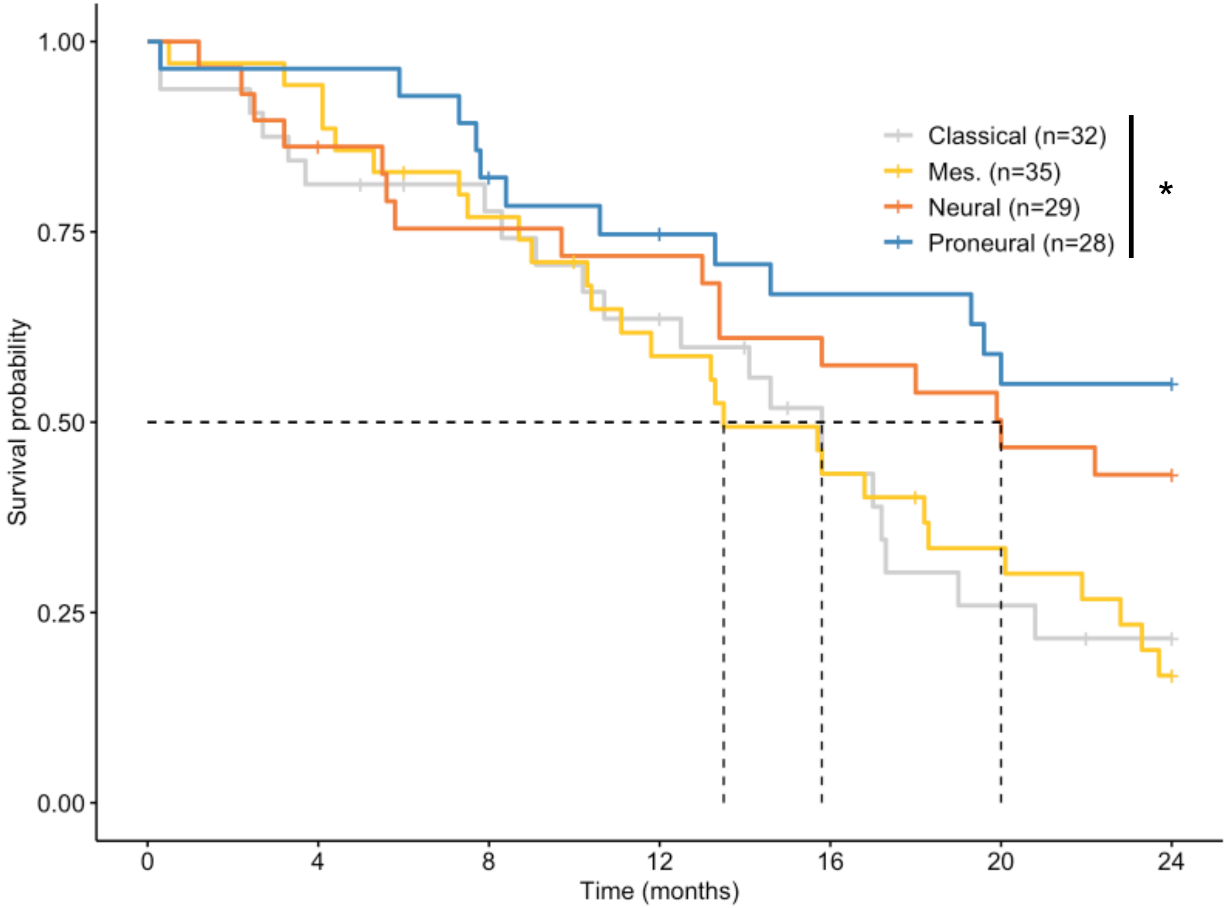

Supplementary Figure 11: Kaplan-Meier curves modeling the effect of GBM molecular classification on survival in the validation cohort.

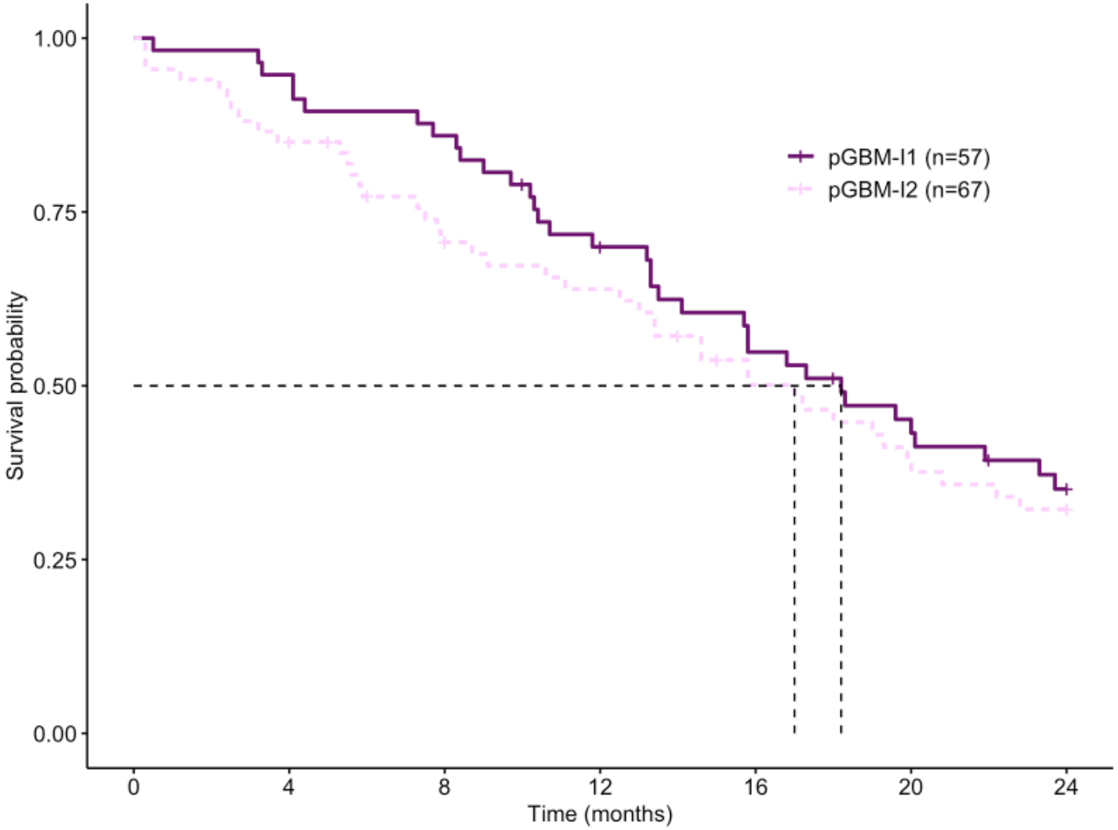

Supplementary Figure 12: Kaplan-Meier curves modeling the effect of tumor infiltration on overall survival in the validation cohort.

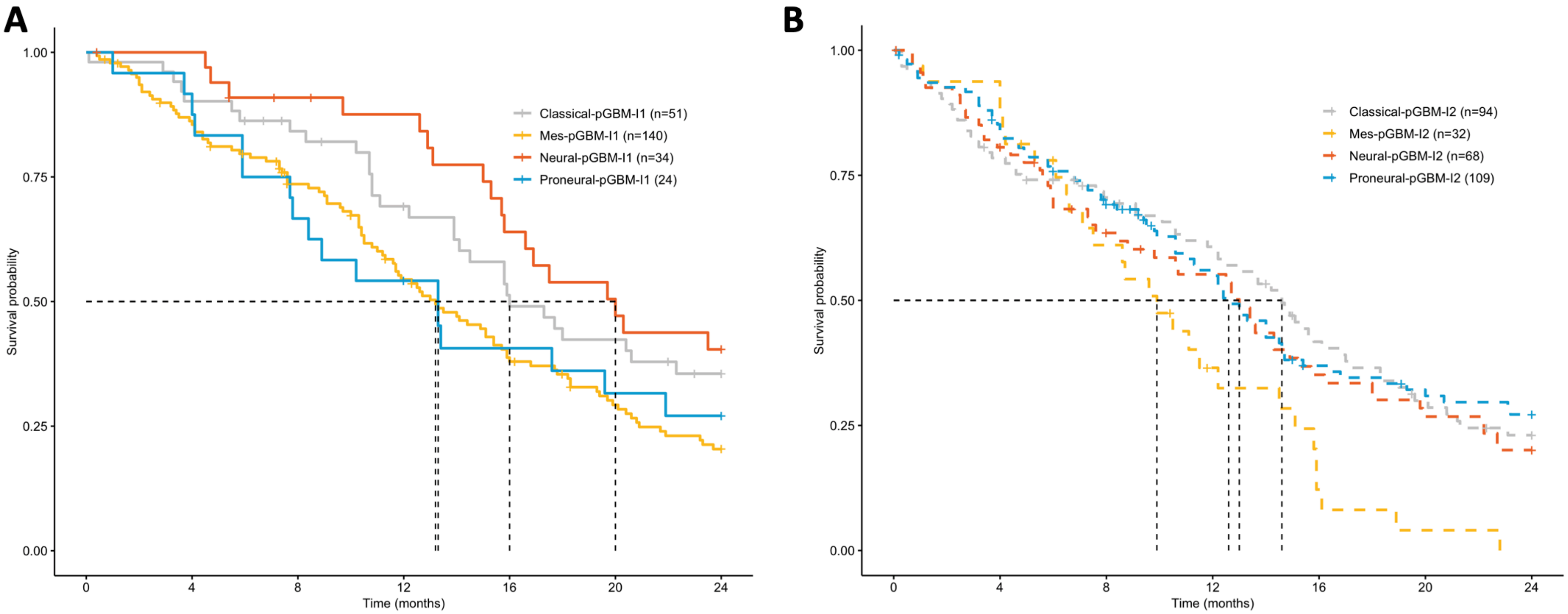

Supplementary Figure 13: Effect of molecular subtypes on survival, in the pooled exploratory and validation cohorts, in (A) pGBM-I1 and (B) pGBM-I2.